Polymethyl methacrylate UV aging: numerical modeling and experimental validation

Aghilas HANNOU[1,*], Rabah FERHOUM[1], Marzak ZEROUKI[1], Madjid ALMANSBA[1]
[1]*Laboratoire (LEC2M), Université Mouloud Mammeri de Tizi-Ouzou, Algérie.*
Corresponding author: aghiiil2013@hotmail.fr*
Received: 15 October, 2024; Accepted: 02 December, 2024; Published: 27 January, 2025

Abstract

This work focuses on the experimental study and numerical modeling of the effect of UV aging on the macroscopic and microscopic behavior of Polymethyl Methacrylate (PMMA). The PMMA specimens, elaborated with the plastic molding process, were exposed to UV radiation in a chamber for two aging times: 120h and 250h. Thereafter, the specimens before and after exposures to UV radiation were visually analyzed and weighed on an analytical balance. Compression tests were carried out on the specimens with a strain rate of 10-3s-1. The effect of UV radiation on PMMA specimens was manifested at the macroscopic scale by: yellowing of the specimens, loss of mass, and decrease of some mechanical properties such as Young's modulus, and at the microscopic scale by breaking the c=o chains. UV aging was modeled by introducing mass loss into Young's modulus values. The model was implemented in the finite element code using the VUMAT subroutine. Simulations were conducted on PMMA specimens with different periods of exposure to UV radiation. Comparisons with experimental results demonstrated the capability of the implemented model to simulate the UV aging effect.

Keywords *: Polymethyl Methacrylate (PMMA), UV aging, VUMAT, Abaqus/Explicit*

I. Introduction

Due to their good specific mechanical properties and ease of processing, the application of industrial polymeric materials has considerably increased. The use of PMMA materials presents many advantages due to their low cost and their generally good mechanical properties, their low production cost, and their low density. They are used in all industry sectors, either as structural materials (aeronautics, cars, etc.) or as insulating materials (electronics and electrical engineering.

Plastics occupy a prominent place in our environment and are now present everywhere, PMMA is one of them. Since it is a completely amorphous polymer, its glass transition temperature is 105°C; this relatively high temperature allows it to work at a fairly high processing temperature [1] and thus has an exquisite visual appearance. Hence its major use outdoors, these materials degrade when exposed to temperature variations, rain or sunlight, and water or oils.

A wealth of literature has been reported on the degradation mechanisms of PMMA [2-5]. It is well recognized that ultraviolet (UV) irradiation causes significant physicochemical changes in polymers, resulting in a decrease in their mechanical performance through a drop in masse weights [6].

II.1 Background on photodegradation

Degradation of polymers significantly affects their mechanical behavior and the evolution of their microstructure. Two types of process can be distinguished, chemical (chain breaking) and physical (mass loss, and both strongly related). The degradation may be, for example, induced by physico-chemical attacks (water, oxygen, etc.), temperature, mechanical stress, and UV irradiation. The degradation mechanisms depend on the type of polymer (amorphous, semi-crystalline,…etc.) and the environment (temperature, chemical medium….etc.).

In general, these mechanisms are controlled by a variety of factors, including diffusion processes (e.g. diffusion of oxygen and/or water), the polymer morphology, and the concentration of impurities in the polymer.

In the last decades, many studies have reported that in many thermoplastic polymers such as polypropylene, polycarbonate, and PMMA, when exposed to Ultraviolet light, the primary structure undergoes considerable modifications due to chain scission and the creation of molecular defects such as carbonyl groups and crosslinking [7-9].

Polycarbonate (PC) subjected to UV irradiation shows important modifications in the optical properties by reducing its transparency and microhardness through the thickness proving a gradual deterioration in the depth [7]. Shyichuk et al., 2001; Craig et al., 2005 [10, 11] confirmed that when Polypropylene (PP) is exposed to UV radiation, the size of

the crystalline domains changes significantly, and chain scission events cause chain segments in the amorphous phase to become untangled, which improves crystallisability.
The mechanical characteristics of PLA decrease due to photodegradation. In particular, a loss of stiffness and strength was observed by S. Belbachir and al (2008) [12]. Ho and Pometto (1999) [13] and Ho et al. (1999) [14] demonstrate that prolonged exposure to UV light reduces the molecular weights and mechanical characteristics of PLA films, such as the young modulus, stress, and strain at break.

II.2 Scope of this work

This work is divided into two parts: the first part is experimental, which consists of studying the impact of aging by UV radiation on the behavior of PMMA. The second part is numerical which consists of modeling the effect of UV irradiation on the elastic–viscoelastic behavior of amorphous PMMA. A semi-phenomenological model able to capture the finite strain behavior of PMMA is elaborate to predict the photodegradation effect on the overall stress-strain response. Several models were elaborated and developed to describe the elastic–viscoelastic deformation of polymers [15-28].
In this study, the effect of degradation by UV radiation is introduced in Young's modulus as a function of mass loss. The model was implemented in the Abaqus/explicit finite element code using the VUMAT subroutine. Uni-axial compression simulations were conducted at different exposure times to UV radiation. The numerical results were compared with the experimental results.
The various experiments carried out in the present work have revealed the effect of UV radiation on the macroscopic and microscopic behavior of PMMA specimens. A loss of mass is observed after many hours under UV radiation. The degradation of the mechanical properties of PMMA such as the Young's modulus was noted. The comparisons between numerical predictions and experimental results demonstrated the capability of the implemented model to match the experimental results.

III. Results and discussion

III.1 Transparency

Figure 2 shows an increase in the yellowing aspect and a decrease in transparency of the irradiation PMMA, as the UV exposure time increase. This yellowing is the result of a chemical reaction caused by UV radiation. The UV energy absorbed by PMMA macromolecules generates a rupture of the most susceptible bonds, which can oxidize in the presence of oxygen. This mechanism is responsible for the formation of substances that cause the yellowing observed in the irradiation samples.

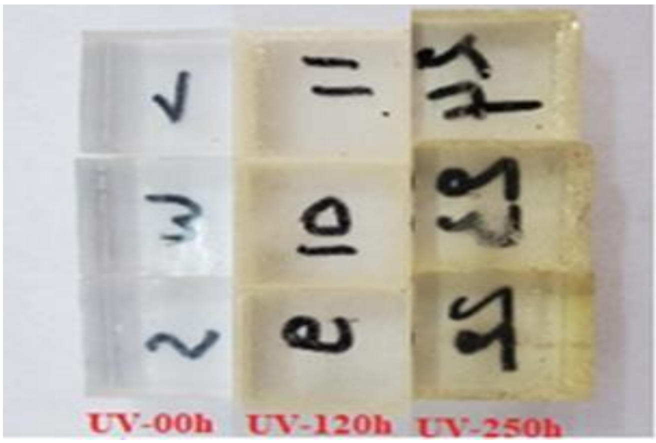

Figure 1: Transparency of the virgin and aged materials

II.2 Weighing measure

The evolution of mass loss as a function of UV exposure time is presented in Figure 2. The decrease in the mass of the specimens was observed with prolonged exposure to UV radiation. At 250h of exposure to UV radiation, the mass of the specimens was dropped from 1.11806g to 1.08534g (-0.03272g), equivalent to a loss of 3% of its initial mass. This loss of mass can be explained by the breaking of molecular chains.

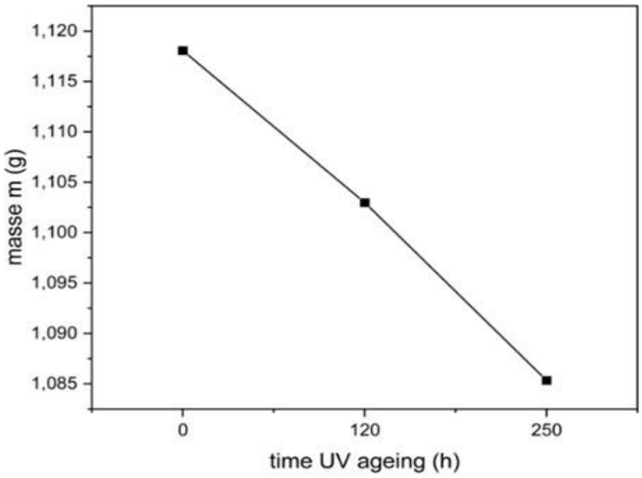

Figure 2: Mass evolution after UV irradiation.

It appears that most of the mechanical properties of PMMA have been affected by the degradation. Indeed, significant changes in Young's modulus (Figure 3).

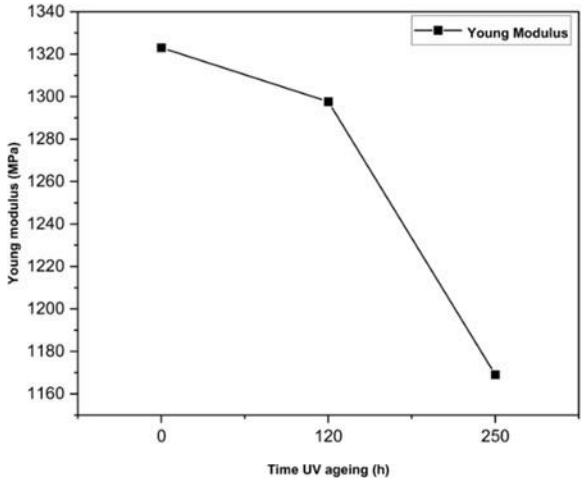

Figure 3: Young Modulus.

III.3 Numerical modeling

The isotropic and symmetric elastic behavior is a Hooke's law that is expressed as a function (1):
(1)

$$\sigma = E.\varepsilon$$

Where σ the elastic stress tensor, ε the elastic strain tensor, and E the Young modulus.

The model developed by Tervoort [29] and modified by Mirkhalaf [26, 30] for thermoplastic materials is described in this section. The plastic strain rate tensor $\dot{\varepsilon}^{vp}$ is given by the equation (2):

$$\dot{\varepsilon}^{vp} = \frac{\sigma^d}{2\chi} \quad (2)$$

Where $\sigma^d$the deviatory part of the stresses is, χ is viscosity function 3 [26, 30-32] is given by:

$$\chi = \varphi_0 \, exp\,(\frac{\Delta H}{RT} + \frac{\mu\sigma^h}{\sigma_0} - \sigma_\infty^{soft}\,\left(1 - exp\,(\frac{-h\sqrt{3}\bar{\varepsilon}^{vp}}{\sqrt{2}\sigma_\infty^{soft}})\right)) \times (\frac{\sigma^{eq}}{sinh\,(\frac{\sigma^{eq}}{\sigma_0})}) \quad (3)$$

The viscosity function depends only on the equivalent plastic strain $\bar{\varepsilon}^{vp}$ defined by equation (4):

$$\bar{\varepsilon}^{vp} = \int_0^t \sqrt{\frac{2}{3}\dot{\varepsilon}^{vp}:\dot{\varepsilon}^{vp}}dt \quad (4)$$

Where σ_0 is a material constant, R is the universal gas constant; T is the constant temperature; ΔH is the activation energy. φ_0 is a pre-exponential factor, is the pressure coefficient. σ_∞^{soft} is the softening parameter and h is The softening slope parameter.

III.4 UV aging equations of the model

Exposure of PMMA to UV radiation causes degradation of the mass and the values of Young's modulus (Figure 3 and Figure 4). This degradation was introduced into the numerical model by adding the effect of mass loss into Young's modulus. The law of Young's modulus degradation is expressed by the following equation (5):

$$E = E_0 - E_t \quad (5)$$

Where E is the degradation value of Young's modulus under UV radiation E_0 expresses the initial value of Young's modulus in the pristine state and E_t presents the value of Young's modulus as a function of the time of exposure to UV radiation and mass loss. It is expressed by equation 6:

$$E_t = E_0.\,exp\,(-\frac{m_t}{m_0})^{\frac{1}{n}} \quad (6)$$

m_t is the mass of the PMMA specimens after each exposure time to ultraviolet (UV) radiation, m_0 is the mass of the specimens without exposure to UV radiation, and n is a parameter depending on the exposure time of the specimens to UV radiation, it acquires values between 0 and 1. After substituting equation 6 into equation 5, we obtained an equation 7:

$$E = E_0.\,(1 - exp\,(-\frac{m_t}{m_0})^{\frac{1}{n}}) \quad (7)$$

Young's modulus condition of the degradation and its implementation will be shown in the figure below (Figure 4).

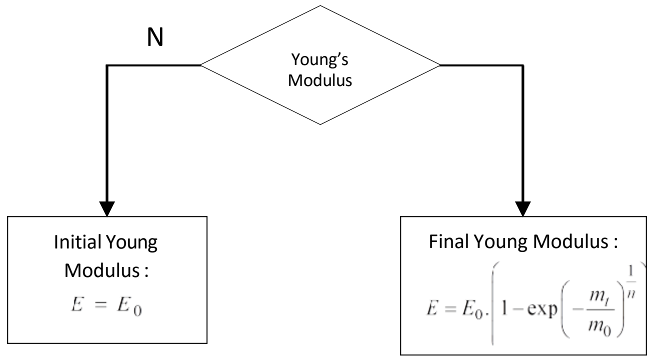

Figure: Diagram of the implementation conditions for the UV degradation

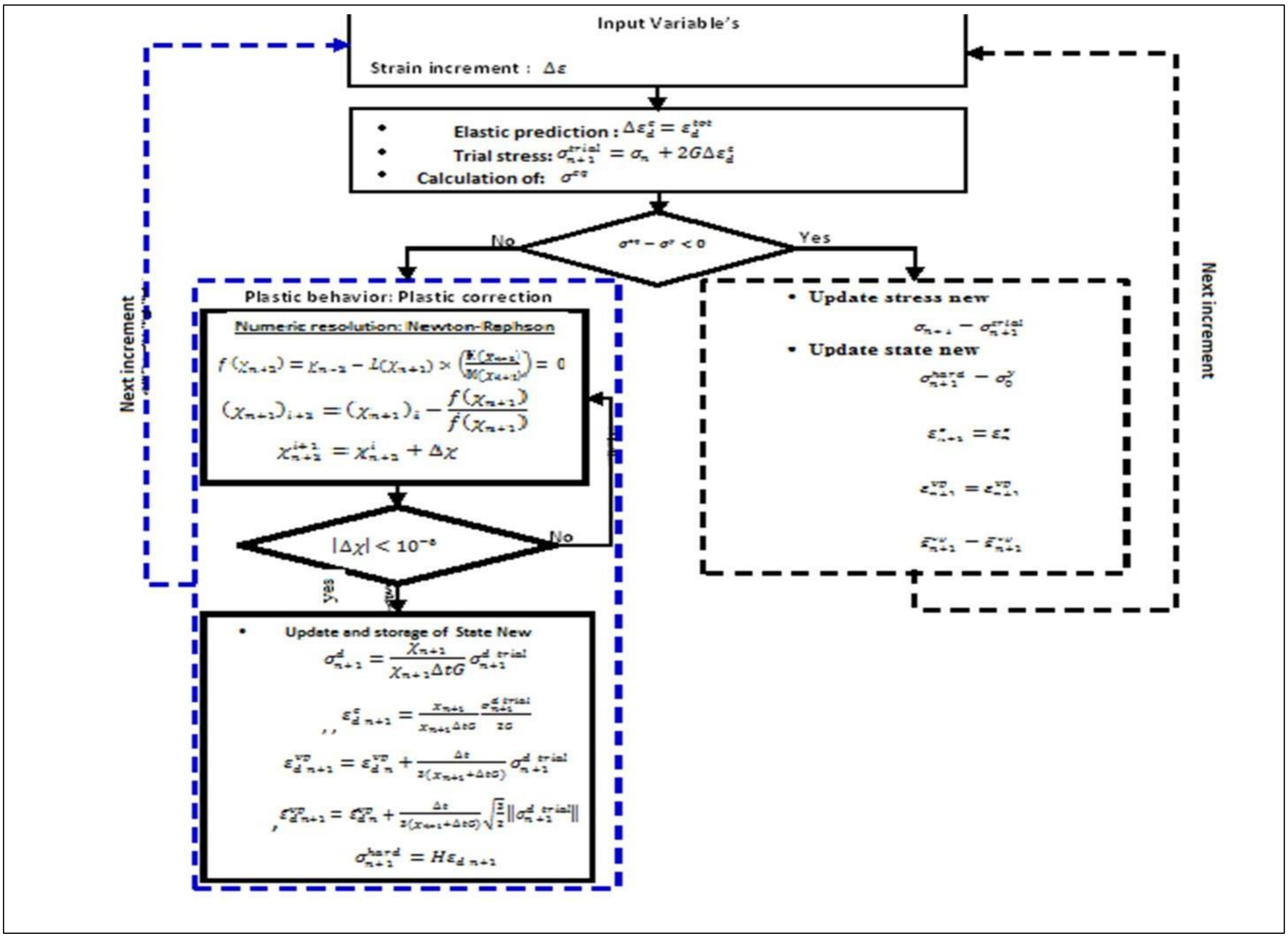

Figure 6: Organigram of the resolution model [31].

The model's equations were solved using the return mapping method. This method is described in detail in Mirakhalef's paper [26]. The model was implemented using the VUMAT subroutine in the Abaqus/Explicit well described in the following figure (Figure 6).

All the details of the development of this model, including the information, approximations, and adjustments to the equations used to ensure its performance in achieving our objective, are reported in the recently published article [31].

III.5 Mesh and Boundary Conditions

Figure 7 gives the boundary conditions imposed on the tested specimens (Dimension: 10x10x6 mm) in axial compression. Le maillage utilisé dans cette étude est de type C3D8R (3D finite element with reduced integration). The bottom rigid body has been fixed in the loading direction and an axial displacement of 2.5 mm has been imposed on the top rigid body.

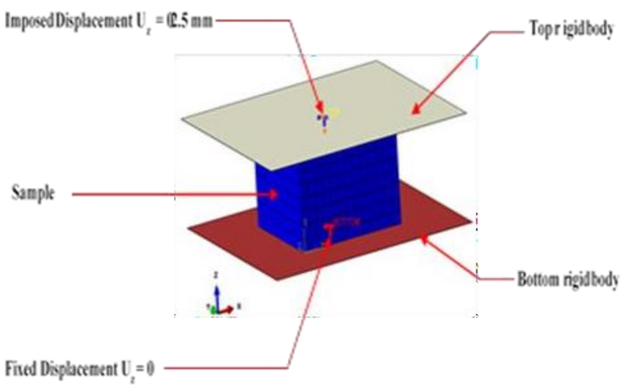

Figure 7: Boundary conditions were applied to the tested specimen

The material parameters used in this work have been listed in Table 1. The values of these parameters have been obtained after a parametric study [26, 30] and [32].

Biopolymer Applications Journal   Aghilas HANNOU et al. Vol 4, N°1, 2025, pp. 17-24
e-ISSN : 2800-1729

Table 1 Elasto-viscoplasticity model parameter's

E_0	υ	σ_0^y	H	σ_0	φ_0	σ_∞^{soft}	h	μ	ΔH	R	n
MPa	/	MPa	MPa	MPa	s				MJ/mol		
2200	0.4	1.95	4.6	00.6517	3.6e-25	29.7	80	0.010	3.e+08	8314.3	0.5

III.5 Numerical and experimental confrontation

In this section, comparisons between the experimental and numerical results have been carried out. Figure 8 illustrates the comparison between the numerical predictions and the experimental results for different exposure times to UV radiation. The implemented model correctly reproduced the behavior of the PMMA specimens under uniaxial compression and for the different UV exposure times. The divergence observed at the level of the maximum stress is explained by some limitations of the implemented model.

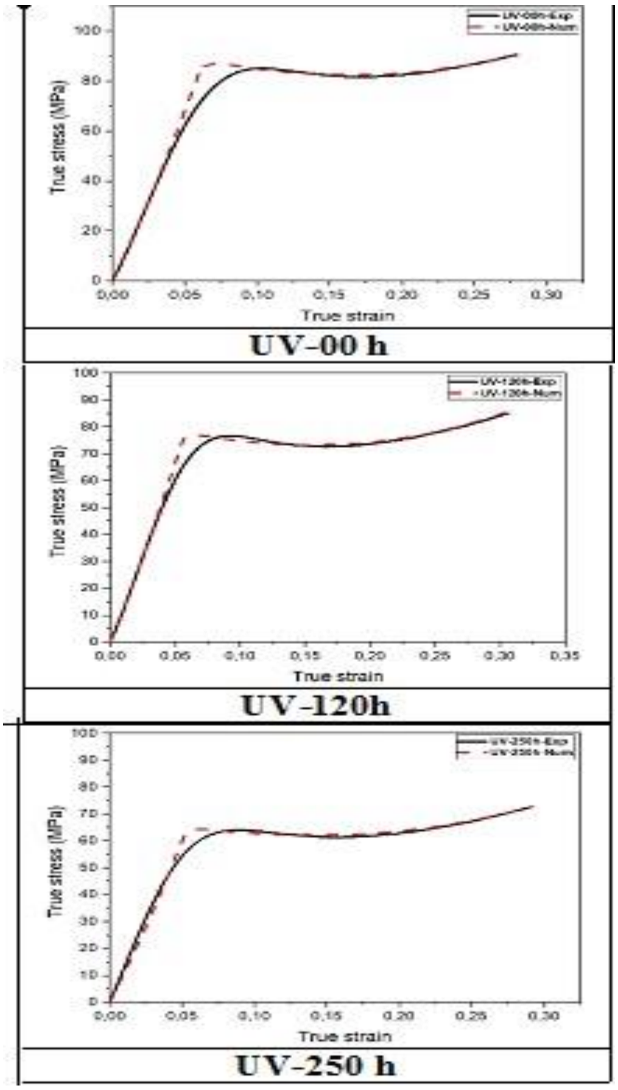

Figure 8: Comparison of true stress-true strain curves for each UV exposure time.

Figure gives the distribution of the von stresses in the PMMA specimens after deformation obtained with the implemented model. The deformation of the specimens is symmetrical and the maximum value of the stresses was reported at the thickness region. The result also shows a physical mesh deformation.

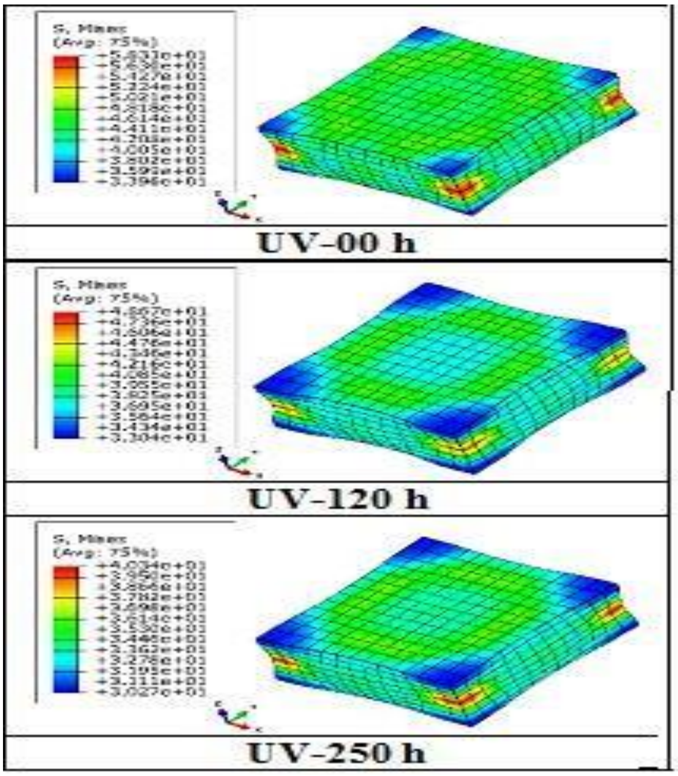

Figure 9: Von Mises stress distribution in the specimens after compression

Erreur ! Source du renvoi introuvable.-a shows the superposition of the true strain-true stress curves obtained by the implemented model. **Erreur ! Source du renvoi introuvable.**-b shows the superposition of the resulting experimental true strain-true stress curves. These superpositions have revealed the effect of the degradation of Young's modulus and the elastic limit introduced in the numerical model.

The comparison between the experimental and numerical degradation of Young's modulus is presented in **Erreur ! Source du renvoi introuvable.**-c. The results obtained show a good consistency between the experimental and numerical values. The degradation relation (equations 7) applied to Young's modulus gives a good prediction of the experimental data.

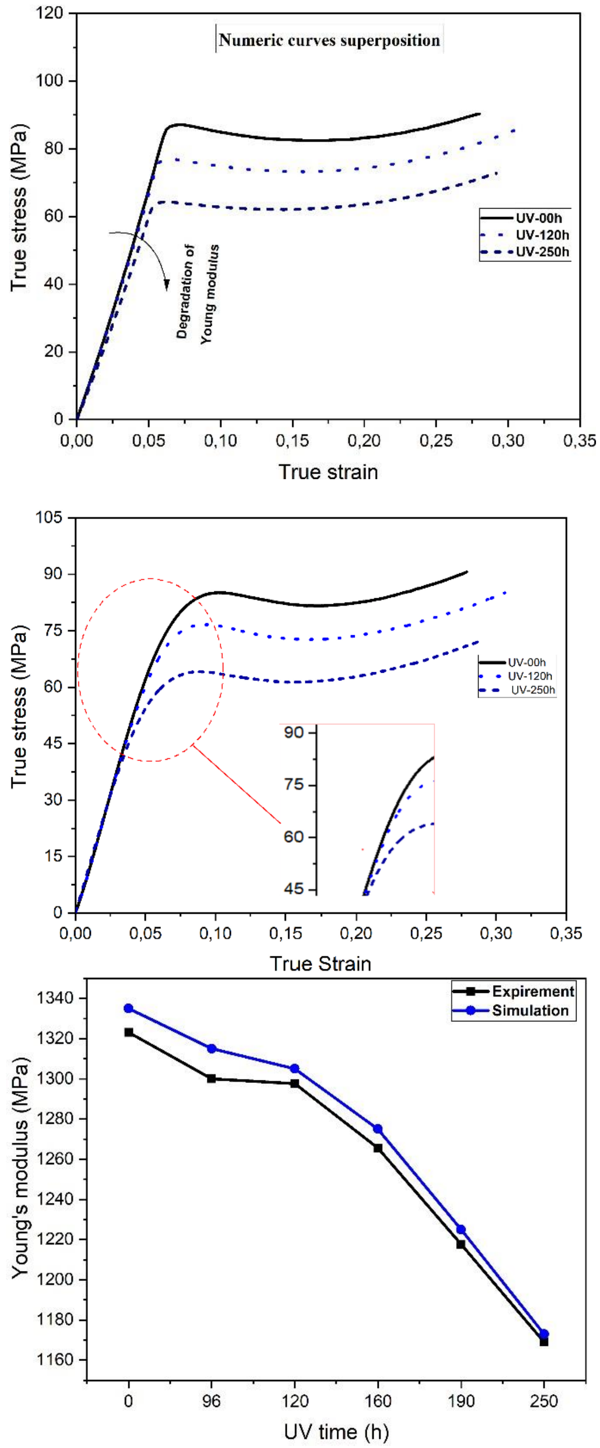

Figure 10: Comparing results for each holds time exposure: (a) numerical true strain-true stress curves, (b) experimental true strain-true stress curves, (c) numerical and theoretical degrading Young's modulus.

IV. Conclusions

Experimental investigations were conducted in this work concerning the effect of UV radiation on the macroscopic and microscopic behavior of PMMA specimens. These specimens were exposed to UV radiation for various hours: 120h and 250h. A series of tests were carried out on the specimens before and after exposure to UV radiation such as the uni-axial compression test. A loss of mass was observed on the specimens exposed to UV radiation. Compression test results revealed that some mechanical properties of PMMA such as Young's modulus and yield strength dropped after exposure to UV radiation. The effect of degradation of Young's modulus was modeled by an exponential law as a function of mass loss. The modified model was implemented in the Abaqus/Explicit finite element code using the VUMAT subroutine. Simulations were carried out on PMMA specimens at different times of exposure to UV radiation. The numerical results obtained were compared with the experimental results. This comparison showed the ability of the implemented model to simulate the effect of Young's modulus degradation. In the future, we plan to extend the Tervoort model to take into account the maximum stress and to carry out experimental investigations on a wide range of polymers.

Nomenclatur

$\bar{\bar{\sigma}}$: Stress tensor, $\bar{\bar{\varepsilon}}$: Strain tensor,
E: the Young modulus
$\dot{\varepsilon}^{v}$: Rate of viscoplastic strain tensor,
σ^{d}: Deviatoric part of the stress tensor,
σ_0 : material constant,
R: Universal gas constant,
T: Constant temperature,
μ: pressure coefficient,
σ^{eq}: Effective or equivalent stress,
σ^{h}: Hydrostatic stress tensor,
σ_{ini} initial yield strength,
υ: Poisson's ratio,
σ_{∞}^{soft}: softening parameter,
h: softening slope parameter,
ΔH: activation energy,
φ_0: Pre-exponential factor,
$\bar{\varepsilon}^{v}$: Equivalent viscoplastic strain,
σ^{hard}: Linear isotropic hardening,
H: Hardening parameter,
ε^{d}: Deviatoric strain,
m_0: mass of the specimens without exposure to UV radiation,
m_t: mass of the PMMA specimens after each exposure time to ultraviolet (UV) radiation,
n: parameter depending on the exposure time of the specimens to UV radiation, it acquires values between 0 and 1.

References:

[1] N. Okhay, *Synthèse de réseaux polymères thermoréversibles par réaction de Diels-Alder*, Saint-Etienne (2012).

[2] S. Li, The influence of the short-term ultraviolet radiation on the structure and properties of poly (p-phenylene terephthalaramide) fibers, Applied surface science, 265, 519-526 (2013).

[3] H. Tsuji, S. Miyauchi, *Poly (L-lactide): VI Effects of crystallinity on enzymatic hydrolysis of poly (L-*

lactide) without free amorphous region. Polymer degradation and stability, 71(3), 415-424 (2001)
[4] G. Bae, T. Park, I.H. Song, *Surface Modification of Polymethylmethacrylate (PMMA) by Ultraviolet (UV) Irradiation and IPA Rinsing.* Micromachines, 2022. **13**(11), 1952 (2022).
[5] H. Tsuji, Y. Ikada, Properties and morphology of poly (L-lactide) 4. Effects of structural parameters on long-term hydrolysis of poly (L-lactide) in phosphate-buffered solution. Polymer degradation and stability, 67(1), 179-189 (2000)
[6] H. Kaczmarek, L. Lindén, J. Rabek, Photo-oxidative degradation of poly (2, 6-dimethyl-1, 4-phenylene oxide) in the presence of concentrated hydroxy peroxide: The role of hydroxy (HO.) and hydroperoxy (HO2.) radicals. Polymer degradation and stability, 47(2), 175-188 (1995)
[7] S. Redjala, UV Aging Effects on Polycarbonate Properties. Journal of Failure Analysis and Prevention, 20(6) 1907-1916 (2020).
[8] J. White, A. Shyichuk, Effect of stabilizer on scission and crosslinking rate changes during photo-oxidation of polypropylene. Polymer degradation and stability, 92(11), 2095-2101 (2007).
[9] S. Redjala, Degradation of polycarbonate properties under thermal aging. Journal of Failure Analysis and Prevention, 19(2), 536-542 (2019)
[10] A. Shyichuk, Quantitative analysis of the temperature effect on the radiation crosslinking and scission of polyethylene macromolecules. Journal of Polymer Science Part A: Polymer Chemistry, 39(10), 1656-1661 (2001).
[11] I. Craig, Photo-induced scission and crosslinking in LDPE, LLDPE, and HDPE. Polymer Engineering & Science, 45(4), 579-587 (2005).
[12] S. Belbachir, Modelling of photodegradation effect on elastic–viscoplastic behaviour of amorphous polylactic acid films. Journal of the Mechanics and Physics of Solids, 58(2), 241-255 (2010).
[13] K.L.G. Ho, A.L. Pometto III, Effects of electron-beam irradiation and ultraviolet light (365 nm) on polylactic acid plastic films. Journal of environmental polymer degradation, 7(2), 93-100 (1999).
[14] K.L.G. Ho, Degradation of polylactic acid (PLA) plastic in Costa Rican soil and Iowa state university compost rows. Journal of environmental polymer degradation, 7(4), 173-177 (1999).
[15] S. Ahzi, Modeling of deformation behavior and strain-induced crystallization in poly (ethylene terephthalate) above the glass transition temperature. Mechanics of materials, 35(12), 1139-1148 (2003).
[16] N.M. Ames, A thermo-mechanically coupled theory for large deformations of amorphous polymers. Part II: Applications. International Journal of plasticity, 25(8), 1495-1539 (2009).
[17] L. Anand, N. Ames, On modeling the micro-indentation response of an amorphous polymer. International Journal of plasticity, 22(6), 1123-1170 (2006).
[18] L. Anand, M.E. Gurtin, A theory of amorphous solids undergoing large deformations, with application to polymeric glasses. International Journal of Solids and Structures, 2003. 40(6), 1465-1487, (2003).
[19] G.Ayoub, A continuum damage model for the high-cycle fatigue life prediction of styrene-butadiene rubber under multiaxial loading. International Journal of Solids and Structures, 48(18), 2458-2466 (2011).
[20] G. Ayoub, Modelling large deformation behaviour under loading–unloading of semicrystalline polymers: application to a high density polyethylene. International Journal of plasticity, 26(3), 329-347 (2010).
[21] D. Bochicchio, G.M. Pavan, Molecular modelling of supramolecular polymers. Advances in Physics: X, 3(1), 1436408 (2018).
[22] M.C. Boyce, E.M. Arruda, Constitutive models of rubber elasticity: a review. Rubber chemistry and technology, 73(3), 504-523 (2000).
[23] M.C. Boyce, D.M. Parks, A.S. Argon, Large inelastic deformation of glassy polymers. Part I: rate dependent constitutive model. Mechanics of materials, 7(1),15-33 (1988).
[24] R. Haward, G. Thackray, The use of a mathematical model to describe isothermal stress-strain curves in glassy thermoplastics. Proceedings of the Royal Society of London. Series A. Mathematical and Physical Sciences, 302(1471), 453-472 (1968).
[25] A. Makradi, A two-phase self-consistent model for the deformation and phase transformation behavior of polymers above the glass transition temperature: application to PET. International Journal of plasticity, 21(4), 741-758 (2005).
[26] S. Mirkhalaf, F.A. Pires, R. Simoes, An elasto-viscoplastic constitutive model for polymers at finite strains: Formulation and computational aspects. Computers & Structures, 166, 60-74 (2016).
[27] A. Adams, C. Buckley, D. Jones, Biaxial hot drawing of poly (ethylene terephthalate): measurements and modelling of strain-stiffening. Polymer, 41(2), 771-786 (2000).
[28] R. Ferhoum, M. Aberkane, K. Hachour, Analysis of thermal ageing effect (hold time-crystallinity rate-mechanical property) on high density polyethylene (HDPE). International Journal of Materials Science and Applications, 2(3), 109 (2014).
[29] T. Tervoort, A constitutive equation for the elasto-viscoplastic deformation of glassy polymers. Mechanics of Time-Dependent Materials, 1(3), 269-291 (1997).
[30] S. Mirkhalaf, F.A. Pires, R. Simoes, Modelling of the post yield response of amorphous polymers under different stress states. International Journal of plasticity, 88, 159-187 (2017)

[31] A. Hannou, Thermal Aging Effect on the Compression Behavior of Thermoplastic Polymers—Proposed Phenomenological Model. Journal of Failure Analysis and Prevention, (2023).

[32] A. Hannou, R. Ferhoum, M. Almansba, Thermal aging effect on the mechanical behavior of polycarbonate: Experimental and modeling. Materials Today: Proceedings, 53, 202-208 (2022).